Cell Motion Model for Moving Dielectrophoresis

ARTICLE *in* ANALYTICAL CHEMISTRY · AUGUST 2008

Impact Factor: 5.64 · DOI: 10.1021/ac800947e · Source: PubMed

5 AUTHORS, INCLUDING:

Chun Yang
Nanyang Technological University
236 PUBLICATIONS **4,652** CITATIONS
SEE PROFILE

Kamal Youcef-Toumi
Massachusetts Institute of Technology
203 PUBLICATIONS **2,323** CITATIONS
SEE PROFILE

Anal. Chem. **2008,** *80,* 5454–5461

Cell Motion Model for Moving Dielectrophoresis

Chin Hock Kua,[†] Yee Cheong Lam,*[,†,‡] Isabel Rodriguez,[§] Chun Yang,[‡] and Kamal Youcef-Toumi[†,||]

Singapore−MIT Alliance, and School of Mechanical and Aerospace Engineering, Nanyang Technological University, Singapore 639798, Institute of Materials Research and Engineering, Singapore 117602, and Department of Mechanical Engineering, Massachusetts Institute of Technology, Cambridge, Massachusetts 02139

Moving dielectrophoresis has been recently developed by the authors as an alternative method to achieve simultaneous cell fractionation and transportation. With an array of independently excitable microelectrodes, this method generates a moving electric field to sequentially fractionate and transport cells across a microchannel. Due to the peculiarity of this method, the motion of the cells is unsteady and there are interesting and distinct differences between cells experiencing positive or negative dielectrophoresis. For a proper understanding and design of a microdevice utilizing this methodology, this study presents a model for the equation of motion for a polarized cell and its unsteady motion under moving dielectrophoresis. The model considers the basic module to generate a moving electric field, where there is a finite-width top electrode and an infinite-width bottom electrode, in a parallel-plate configuration. The forces considered include dielectrophoretic force, fluid drag, buoyancy, and gravitational force. These forces are modeled as equivalent point forces acting at the center of mass of the cell. A parallel-plate wall correction factor is employed to account for the effect of the large cell size to microchannel height ratio. Various parameters are examined including the initial position of the cell relative to the electrodes, cell's Clausius−Mossotti factor, cell size, applied voltage, electrode width, interelectrode gap, microchannel height, number of energized electrodes, and types of electrode configurations. Reasonable agreements were obtained between simulated and experimental results. As the solution of the unsteady motion is rather tedious, a MATLAB algorithm, with all the associated files, for the prediction of the cell trajectory, is available on request.

Dielectrophoresis has been widely used as a method to achieve cell separation in microfluidic applications. Conventional dielectrophoresis encompasses a nonuniform ac electric field to polarize and separate cells based on their electrical properties, i.e., permittivity and conductivity.[1,2] The traveling wave dielectrophoresis has also been introduced to achieve simultaneous cell separation and transportation and has been demonstrated on biological cells.[3–5] Several innovative cell manipulation techniques have been developed that utilize conventional dielectrophoresis to achieve cell separation, which includes insulator-based dielectrophoresis,[6,7] dc-based dielectrophoresis,[8] and programmable-based dielectrophoresis.[9] Cell separation based on conventional dielectrophoresis is more straightforward in operation as compared to traveling wave dielectrophoresis.

Recently, moving dielectrophoresis has been developed by the authors as an alternative method to achieve simultaneous cell fractionation and transportation.[10] The moving dielectrophoresis achieves cell separation and transportation by sequentially energizing the adjacent microelectrodes. Unlike the traveling wave dielectrophoresis, which requires both the real and imaginary parts of the Clausius−Mossotti factor for its operation, the moving dielectrophoresis utilizes only the real part of the Clausius−Mossotti factor, and thus maintains simplicity in operation similar to that of the conventional dielectrophoresis. Moving dielectrophoresis has been used to demonstrate the fractionation and transportation of viable and nonviable yeast cells.[10] This method employs a single microelectrode or an array of independently excitable microelectrodes to generate a nonuniform electric field that travels sequentially in a controlled manner along the microchannel; see Figure 1. Due to the peculiarity of this method, the motion of the cells is unsteady, and there are interesting and distinct differences between cells experiencing positive or negative dielectrophoresis. For a proper understanding and design of a microdevice utilizing this methodology, the underlying mechanism can be demonstrated by considering its basic module, i.e., a finite-width top electrode and an infinite-width bottom electrode, in a parallel-plate configuration. A model is presented in this study that captures

* To whom correspondence should be addressed. E-mail: myclam@ntu.edu.sg.
† Singapore-MIT Alliance, Nanyang Technological University.
‡ School of Mechanical and Aerospace Engineering, Nanyang Technological University.
§ Institute of Materials Research and Engineering.
|| Massachusetts Institute of Technology.

(1) Pohl, H. A. *Dielectrophoresis: The behavior of neutral matter in nonuniform electric fields*; Cambridge University Press: New York, 1978.
(2) Morgan, H.; Green, N. G. *AC Electrokinetics: colloids and nanoparticles*; Research Studies Press: Philadelphia, 2003.
(3) Huang, Y.; Wang, X.-B.; Tame, J. A.; Pethig, R. *J. Phys. D: Appl. Phys.* **1993**, *26*, 1528–1535.
(4) Gascoyne, P. R. C.; Huang, Y.; Hughes, M. P.; Wang, X.-B.; Pethig, R.; Becker, F. F. *IEEE Eng. Med. Biol. Soc.* **1994**, *16*, 772–773.
(5) Talary, M. S.; Burt, J. P. H.; Tame, J. A.; Pethig, R. *J. Phys. D: Appl. Phys.* **1996**, *29*, 2198–2203.
(6) Lapizco-Encinas, B. H.; Simmons, B. A.; Cummings, E. B.; Fintschenko, Y. *Anal. Chem.* **2004**, *76*, 1571–1579.
(7) Iliescu, C.; Xu, G.; Loe, F. C.; Ong, P. L.; Tay, F. E. H. *Electrophoresis* **2007**, *28*, 1107–1114.
(8) Kang, K. H.; Kang, Y.; Xuan, X.; Li, D. *Electrophoresis* **2005**, 26.
(9) Chiou, P. Y.; Ohta, A. T.; Wu, M. C. *Nature* **2005**, *436*, 370–372.
(10) Kua, C. H.; Lam, Y. C.; Rodriguez, I.; Yang, C.; Youcef-Toumi, K. *Anal. Chem.* **2007**, *79*, 6975–6987.

10.1021/ac800947e CCC: $40.75
Published on Web 06/18/2008

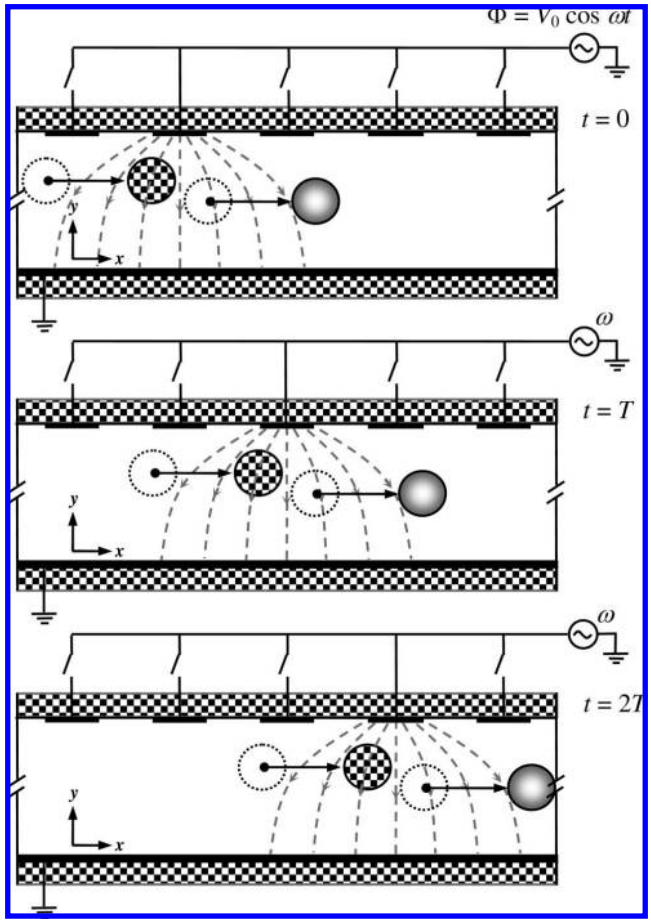

Figure 1. Illustration of cell manipulation using moving dielectrophoresis. Hatched circle and solid circle represent cells experiencing positive and negative dielectrophoretic forces, respectively. Moving electric field is generated by sequentially energizing single (or array of) electrodes to form an electric field that moves from one end to other. At time $t = 0$, cell experiencing positive dielectrophoresis is attracted to the energized electrode. At time $t = T$, the same cell moves to the third electrode. By sequentially applying an electric field with an angular frequency ω that moves from left to right with a tempo T, the same cell is sequentially attracted to the energized electrode. In contrast, cell experiencing negative dielectrophoretic force is sequentially repelled on each successive step. The dotted circles represent the initial positions of the cells.

the equation of motion for a cell under such basic module, and the effects of various parameters on the cell's trajectory are discussed.

Calculating the trajectory of a cell from the equation of motion requires summing the forces acting on the cell. There are many methods to calculate these forces. A rigorous approach is to use surface/volume integral methods to sum all the stress or pressure components on the cell. For example, in the particulate flow problem, the distributed Lagrange multiplier (DLM) method has been used to calculate the particle motion in a fluid and has been demonstrated on the sedimentation problem of sphere.[11,12] The DLM method has also been combined with dipole dielectrophoretic force method to simulate the trajectory of a cell under a traveling wave electric field.[13] The Lattice−Boltzmann method has been used to calculate the hydrodynamic force acting on a sphere that settles in orthogonal cylindrical or prismatic enclosures.[14] These methods take into account the finite size of particles and wall effect directly in solving the particulate flow problems. However, the surface/volume integral methods are complicated and require significant computational power.

The surface and volume forces can also be represented as equivalent point forces. In this method, the surface and volume forces are represented as equivalent forces that act on a point, which is typically the center of mass. This method is convenient for the calculation of the trajectory of a cell as governed by the equation of motion. In this study, the equivalent point forces approach has been adopted, where all the forces acting on a cell are represented as equivalent point forces that act at the center of the cell. In addition, a parallel-plate wall correction factor is employed to account for the large cell size to microchannel height ratio. However, to elucidate the characteristics of the moving dielectrophoresis method, it is insufficient to obtain only the forces acting on a cell. The trajectory of a cell as a function of time has to be obtained through its equation of motion, which has not been attempted previously.

MODEL FOR MOVING DIELECTROPHORESIS

Forces Acting on a Single Cell. The electrode structure shown in Figure 2a is the basic module for generating a moving electric field. Such basic module consists of two parallel plates. The bottom plate has a homogeneous electrode coated on the entire surface. The top plate carries a finite half-electrode of length $1/2d$. The system is symmetric about the y-axis. The z-dimension is significantly larger than the x- and y-dimensions. This system can be treated as two-dimensional dependent on the x- and y-coordinates. The electrodes are excited with a sinusoidal voltage with amplitude V_0 and angular frequency ω.

Suspended in a fluid medium in the microchannel and polarized by the electric fields, a cell experiences a dielectrophoretic force $\mathbf{F}_{DEP}$ that makes the cell move along the microchannel. The four dominant forces acting on the cell are the dielectrophoretic force $\mathbf{F}_{DEP}$, the fluid drag $\mathbf{F}_{drag}$, the buoyancy force $\mathbf{F}_{buoy}$, and the gravitational force $\mathbf{F}_{grav}$. The trajectory of a cell in the microchannel can be obtained by balancing all these forces acting on the cell. Although these forces are exerted either on the surface or the volume of the cell, these forces can be described as equivalent point forces acting on the center of the cell. These assumptions allow the equation of motion for the cell to be simplified without losing generality. These forces can be represented in their x- and y-components as F_{DEP_X}, F_{DEP_Y}, F_{drag_X}, F_{drag_Y}, F_{buoy}, and F_{grav}; see Figure 2a.

According to Newton's law of motion, the rate of change in the momentum of a cell is directly proportional to the sum of the forces acting on the cell, which can be represented as a system of two differential equations in the x- and y-directions, respectively,

$$F_{DEP\_X} - F_{drag\_X} = m \frac{d^2x}{dt^2} \quad (1)$$

(11) Glowinski, R.; Pan, T.-W.; Hesla, T. I.; Joseph, D. D. *Int. J. Multiphase Flow* **1999**, *25*, 755–794.
(12) Singh, P.; Joseph, D. D.; Hesla, T. I.; Glowinski, R.; Pan, T.-W. *J. Non-Newtonian Fluid Mech.* **2000**, *91*, 165–188.
(13) Nudurupati, S.; Aubry, N.; Singh, P. *J. Physics D: Appl. Phys.* **2006**, *39*, 3425.
(14) Feng, Z.-G.; Michaelides, E. E. *Int. J. Multiphase Flow* **2002**, *28*, 479–496.

$$F_{DEP\_Y} - F_{drag\_Y} + F_{buoy} - F_{grav} = m\frac{d^2y}{dt^2} \quad (2)$$

where m is the cell mass and t is time.

We have assumed that other forces such as electrohydrodynamic force,[15–17] electrothermal effect,[18,19] Columbic force, electrical double layer effect, and Brownian motion have minimal effect on the cell motion. This assumption is reasonable for a relatively large and neutral particle like a cell, immersed in a relatively low medium conductivity and operating at the appropriate ac frequency, where the dielectrophoretic force is the dominant force.

Dielectrophoretic Force. The calculation of the dielectrophoretic force involves solving the Laplace's equation for a boundary value problem to obtain the electrical potential and the electric field. This calculation can be performed analytically or numerically. In general, an analytical approach is mathematically involved. Green's theorem[20] and Fourier series[21] have been used to obtain analytical solutions for simple electrode arrays and interdigitated electrode arrays. Alternatively, a numerical approach provides fast solution for almost any electrode configurations. The finite element method[22] and the weighted least-squares finite difference scheme[23] have been used to obtain numerical solutions for two-phase electrode arrays and interdigitated electrode arrays.

In this study, a numerical approach is employed. The governing equations for the dielectrophoretic force are derived from the electromagnetic field, where the unknown is the electrical potential Φ in the xy-space, given the boundary conditions at the bounding edges. In a microfluidic device, the electric field wavelength is typically several orders of magnitude larger than the cell or electrode size. Thus, the electroquasistatic approximation can be used. This assumption allows the time-dependent problem in Figure 2a to be analyzed as a static problem, where the boundary condition $\Phi = V_0 \cos \omega t$ is analyzed as $\Phi = V_0$. Note that although the time-averaged potential is $V_0/\sqrt{2}$, this time-average information is generally embedded in the dielectrophoretic force calculation, and the simulation is performed as though it is a static case of V_0. Since the dielectrophoretic force is dependent on the gradient of the electric field square, $\nabla|\mathbf{E}|^2$, rather than the absolute value of the potential at the boundaries, the potential at the boundaries may take any values as long as their relative difference in value remains the same; i.e., the potential difference between the top and the bottom electrodes remains as V_0.

Applying the electroquasistatic assumptions to the Maxwell equations, and assuming no free charges in the space, the Gauss law reduces to[24]

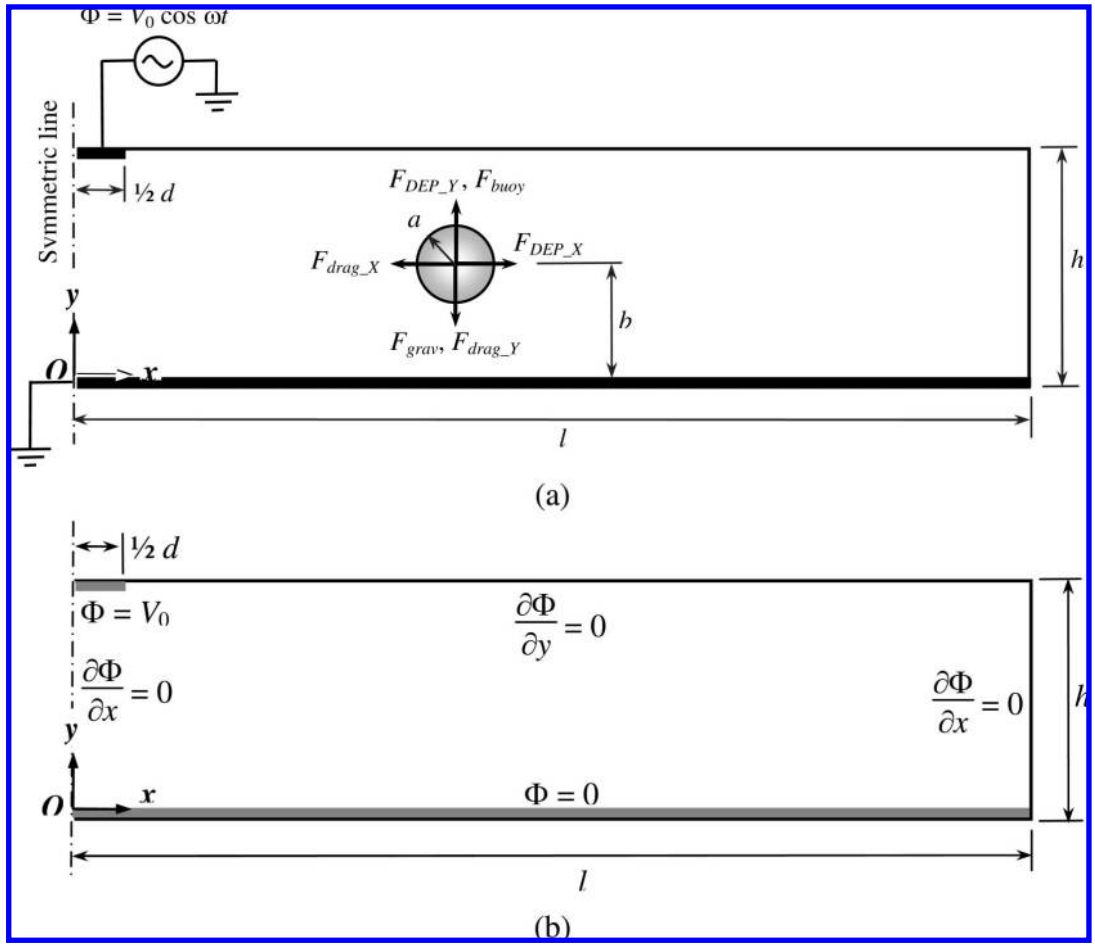

Figure 2. (a) Components of forces acting on a cell in a microchannel under dielectrophoretic and other forces. F_{DEP_X} and F_{DEP_Y} are x- and y-components of dielectrophoretic force, respectively; F_{drag_X} and F_{drag_Y} are x- and y-components of fluid drag, respectively; F_{grav} is the gravitational force; and F_{buoy} is the buoyancy force. (b) Geometries and boundary conditions for the analysis of the electrical potential, the electric field, and the spatial strength of the dielectrophoretic force.

$$\nabla \cdot \nabla \Phi = 0 \quad \text{or} \quad \nabla^2 \Phi = 0 \tag{3}$$

Equation (3) is the governing equation for the electrical potential Φ in the *xy*-space. The electric field **E** is found by taking the gradient of the potential,

$$\mathbf{E} = -\nabla \Phi \tag{4}$$

For the geometry shown in Figure 2a, the top and bottom plates are made of glass. The structure is symmetric at the left edge. Physically, the right edge goes to infinity, but the distance of the right edge from the symmetric line can be approximated as a finite distance l according to the Saint-Venant's principle,[25] as long as l is at least one characteristic length longer than d and h. The microchannel is filled with a fluid medium. The electrical potential is applied on the top and bottom electrodes. Since the electrode thickness is typically less than 100 nm, which is significantly smaller than the microchannel height of at least 20 μm, it is reasonable to model the electrodes as having a zero thickness. These physical conditions translate into boundary conditions shown in Figure 2b.

Assuming that a finite-sized polarized cell can be represented as an equivalent dipole,[26] the time-averaged dielectrophoretic forces in the *x*- and *y*-directions, respectively, acting on a spherical cell with radius a and suspended in a medium with permittivity ε_m are given by[2]

$$F_{DEP\_X} = \pi \varepsilon_m a^3 Re[\tilde{f}_{CM}] \frac{\partial}{\partial x} |\mathbf{E}|^2 \tag{5}$$

$$F_{DEP\_Y} = \pi \varepsilon_m a^3 Re[\tilde{f}_{CM}] \frac{\partial}{\partial y} |\mathbf{E}|^2 \tag{6}$$

where $Re\,[\tilde{f}_{CM}]$ is the real part of the Clausius−Mossotti factor. The $\pi \varepsilon_m a^3 Re[\tilde{f}_{CM}]$ term on the right-hand side of eqs 5 and 6 is a constant for a specific cell and surrounding medium. Only the $\partial|\mathbf{E}|^2/\partial x$ and $\partial|\mathbf{E}|^2/\partial y$ terms determine the spatial strength of the dielectrophoretic force for a specific electrode configuration. For a simple sphere, the Clausius−Mossotti factor $\tilde{f}_{CM}$ is defined as,

$$\tilde{f}_{CM} = \frac{\tilde{\varepsilon}_c - \tilde{\varepsilon}_m}{\tilde{\varepsilon}_c + 2\tilde{\varepsilon}_m} \tag{7}$$

where $\tilde{\varepsilon}_c$ and $\tilde{\varepsilon}_m$ are the complex permittivity of the cell and the suspending medium, respectively. The complex permittivity is defined as $\tilde{\varepsilon} = -i\sigma/\omega$, where ε is the relative permittivity, σ is the conductivity, and ω is the angular frequency. For biological cells, typically a two-shell model[27] is employed to describe their $\tilde{f}_{CM}$ value. The value of the Clausius−Mossotti factor is between −0.5 and 1.0.

Assuming microchannel length of 100 μm, microchannel height of 25 μm, electrode width of 10 μm, and voltage of 5 V, the boundary value problem as illustrated in Figure 2b is solved using finite element simulation software (FlexPDE 5.0 Professional version) to obtain the spatial values of $\partial|\mathbf{E}|^2/\partial x$ and $\partial|\mathbf{E}|^2/\partial y$ terms. These values are then multiplied with the $\pi \varepsilon_m a^3 Re[\tilde{f}_{CM}]$ term to determine the dielectrophoretic force. Figure 3 shows the simulation results for the electrical potential, the magnitude of the electric field, and the magnitude of the gradient of electric field square. Since the gradient of the electric field square represents the spatial strength of the dielectrophoretic force, the result in Figure 3c shows that the dielectrophoretic force decays exponentially away from the top electrode. This force reduces by an order of magnitude for approximately every 20 μm.

Fluid Drag. For a spherical cell moving slowly in a viscous fluid, the fluid drag acting on the cell is proportional to the drag coefficient $6\pi\eta a$ and the cell velocity.[28] For the configuration shown in Figure 2a, a wall correction factor has to be applied to the drag relation since the cell movement is bounded by two

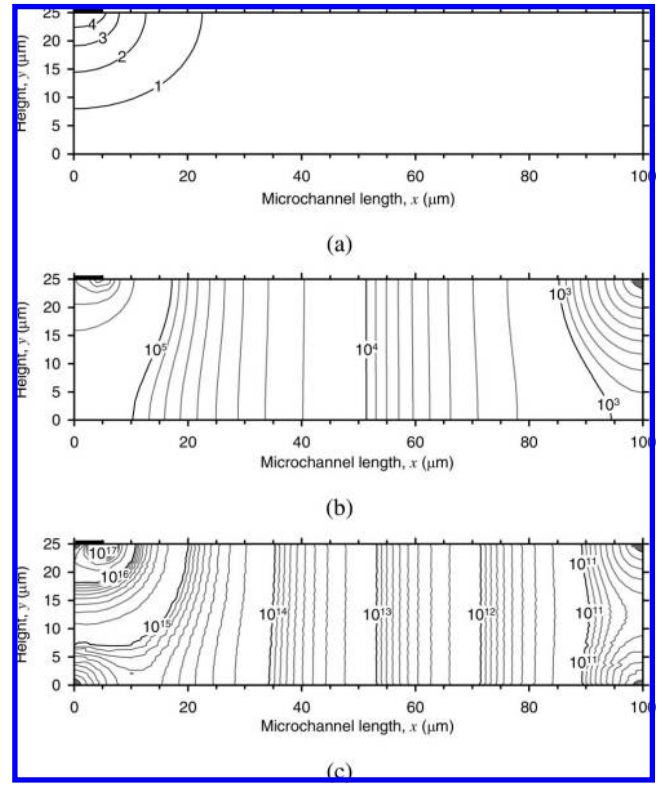

Figure 3. Simulation results for (a) potential, Φ (unit V), (b) magnitude of electric field, **E** (unit V/m), and (c) magnitude of gradient of electric field square, $\nabla|\mathbf{E}|^2$ (unit V^2/m^3).

(15) Castellanos, A.; Ramos, A.; González, A.; Green, N. G.; Morgan, H. *J. Phys. D: Appl. Phys.* **2003**, *36*, 2584–2597.
(16) Jones, T. B. *Nanobiotechnol., IEE Proc.* **2003**, *150*, 39–46.
(17) Ramos, A.; Morgan, H.; Green, N. G.; Castellanos, A. *J. Physics D: Appl. Phys.* **1998**, *31*, 2338–2353.
(18) Green, N. G.; Ramos, A.; Gonzalez, A.; Castellanos, A.; Morgan, H. *J. Electrost.* **2001**, *53*, 71–87.
(19) Tay, F. E. H.; Yu, L.; Pang, A. J.; Iliescu, C. *Electrochim. Acta* **2007**, *52*, 2862–2868.
(20) Wang, X.-J.; Wang, X.-B.; Becker, F. F.; Gascoyne, P. R. C. *J. Phys. D: Appl. Phys.* **1996**, *29*, 1649–1660.
(21) Morgan, H.; Izquierdo, A. G.; Bakewell, D.; Green, N. G.; Ramos, A. *J. Phys. D: Appl. Phys.* **2001**, *34*, 1553–1561.
(22) Green, N. G.; Ramos, A.; Morgan, H. *J. Electrost.* **2002**, *56*, 235–254.
(23) Chen, D. F.; Du, H.; Li, W. H.; Shu, C. *J. Micromech. Microeng.* **2005**, *15*, 1040–1048.
(24) Haus, H. A.; Melcher, J. R. *Electromagnetic Fields and Energy*; Prentice Hall: Englewood Cliffs, NJ, 1989.
(25) Cook, R. D. *Finite Element Modeling for Stress Analysis*; John Wiley & Sons, Inc.: New York, 1995.
(26) Jones, T. B. *Electromechanics of Particles*; Cambridge University Press: New York, 1995.

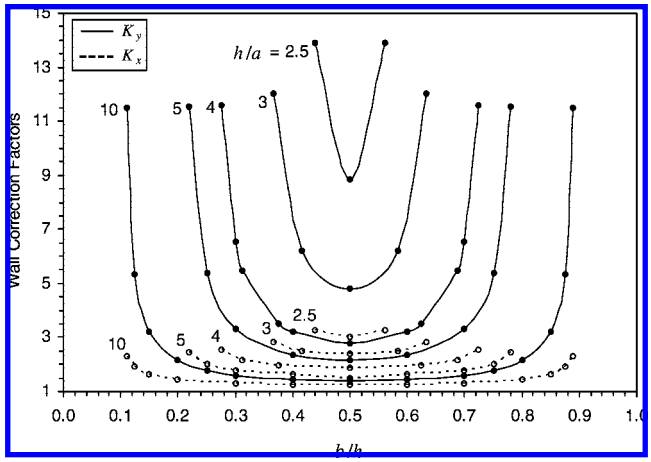

Figure 4. Wall correction factor of fluid drag for a spherical cell in a parallel plate channel in the *x*-direction, K_x and in the *y*-direction, K_y, respectively (*a*, sphere radius; *h*, microchannel height; *b*, distance between center of the sphere to the bottom of the microchannel). These values are adapted from Ganatos.[29]

parallel plates of finite distance apart. The fluid drags on the cell in the *x*- and *y*-directions are, respectively,[29–31]

$$F_{drag\_X} = 6\pi\eta a K_x \frac{dx}{dt} \tag{8}$$

$$F_{drag\_Y} = 6\pi\eta a K_y \frac{dy}{dt} \tag{9}$$

where a is the cell radius, η is the viscosity of the fluid medium, K_x and K_y are the wall correction factors in the *x*- and *y*-directions, respectively, and dx/dt and dy/dt are the instantaneous cell velocities in the *x*- and *y*-directions, respectively. The wall correction factors depend on the ratio of the microchannel height to the cell radius (i.e., h/a) and the ratio of the *y*-position of the cell to the microchannel height (i.e., b/h); see Figure 4. The wall correction factor in the *y*-direction is a few times larger than that in the *x*-direction at a distance near to the wall, which implies that a cell experiences larger resistance in the *y*-directional motion compared to the *x*-directional motion when the cell is moving near to the wall. Thus, a cell tends to stay in a constant elevation when it moves along the microchannel. Since the wall correction factors are only available for certain ratios, the values for other ratios are interpolated from the available values when solving the equation of motion in MATLAB.

Buoyancy and Gravitational Forces. Since a cell fully submerged in a fluid displaces a fluid volume equivalent to the cell's volume, there is a buoyancy force acting on the cell, and such buoyancy force is expressed by

$$F_{buoy} = \rho_m V_p g \tag{10}$$

where ρ_m is the density of the fluid, V_p is the volume of the cell, and g is the gravitational constant.

The gravitational force also acts on the cell, which is given by

$$F_{grav} = mg = \rho_p V_p g \tag{11}$$

where ρ_p is the density of the cell. For a spherical cell, the volume of the cell is given by

$$V_p = \tfrac{4}{3}\pi a^3 \tag{12}$$

These two forces are acting in the *y*-direction; see Figure 2a.

Equation of Motion. Using the *x*-component of the dielectrophoretic force from eq 5 and the fluid drag from eq 8, force balance on the cell in the *x*-direction in eq 1 becomes

$$m\frac{d^2x}{dt^2} = \pi\varepsilon_m a^3 Re[\tilde{f}_{CM}]\frac{\partial}{\partial x}|\mathbf{E}|^2 - 6\pi\eta a K_x \frac{dx}{dt} \tag{13}$$

Using the *y*-component of the dielectrophoretic force from eq 6, the fluid drag force from eq 9, the buoyancy force from eq 10 and the gravitational force from eq 11, force balance on the cell in the *y*-direction in eq 2 becomes

$$m\frac{d^2y}{dt^2} = \pi\varepsilon_m a^3 Re[\tilde{f}_{CM}]\frac{\partial}{\partial y}|\mathbf{E}|^2 - 6\pi\eta a K_y \frac{dy}{dt} + (\rho_m - \rho_p)V_p g \tag{14}$$

Due to the nonsteady nature of the cell motion, the solutions of eqs 13 and 14 for the trajectory of a cell are rather tedious. As such, user-defined computer routines were implemented in MATLAB (version 7 R14, MathWorks) for the solution of these two second-order differential equations to obtain the time-dependent cell trajectories. Since the equations are stiff because the time scale varies greatly across the whole time frame,[32] the trapezoidal rule solver ode23t was used.

SIMULATION

Although the general motion of a cell under dielectrophoretic force may be deduced from the dielectrophoretic force distribution, the solution of the trajectory of a cell under moving dielectrophoresis is not trivial. As shown in Figure 4, a cell experiences a rapidly increasing fluid drag when it travels near the channel wall, as characterized by a rapidly increasing wall correction factor. This counterforce would affect the effectiveness of dielectrophoretic force.

Two representative examples, for cells experiencing positive and negative dielectrophoresis, respectively, have been simulated to provide an understanding of the general behavior of the system. The cell is assumed to have a radius of 2.5 μm and a density of 1040 kg m^{-3}. The fluid is assumed to be a water-based solution, with medium relative permittivity of 78, viscosity of 0.0089 kg m^{-1} s^{-1}, and density of 1000 kg m^{-3}. The free space permittivity and gravitational constant of 8.854×10^{-12} F m^{-1} and 9.81 m s^{-2} were used, respectively.

The first example assumes that the cell has a Clausius−Mossotti factor of 1.0; that is, the cell experiences positive dielectrophoresis.

(27) Huang, Y.; Hölzel, R.; Pethig, R.; Wang, X.-B. *Phys. Med. Biol.* **1992**, *37*, 1499–1517.
(28) Deen, W. M. *Analysis of Transport Phenomena*; Oxford University Press: New York, 1998.
(29) Ganatos, P. Dissertation, The City University of New York, New York, 1978.
(30) Ganatos, P.; Weinbaum, S.; Pfeffer, R. *J. Fluid Mech.* **1980**, *99*, 739–753.
(31) Ganatos, P.; Pfeffer, R.; Weinbaum, S. *J. Fluid Mech.* **1980**, *99*, 755–783.
(32) Shampine, L. F.; Gladwell, I.; Thompson, S. *Solving ODEs with MATLAB*; Cambridge University Press: New York, 2003.

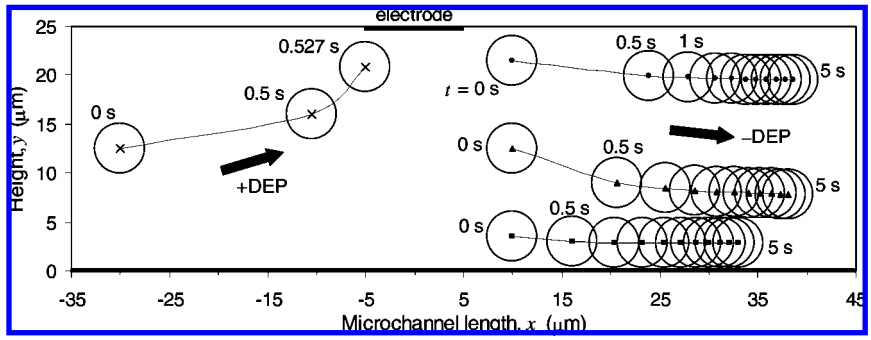

Figure 5. Trajectories of cells experiencing positive dielectrophoresis (+DEP, Clausius−Mossotti factor of 1.0) and negative dielectrophoresis (−DEP, Clausius−Mossotti factor of −0.4), respectively. Initial positions of cells are (−30, 12.5) (×), (10, 3.5) (■), (10, 12.5) (▲), and (10, 21.5) μm (●), respectively. Cell trajectories are plotted with 0.5-s interval, except at point 0.527 s for positive dielectrophoresis. Only one set of data shown for +DEP for clarity.

Simulation is performed using a start time of 0 s, an initial velocity of 0 m s^{-1}, and an initial position of (−30.0, 12.5) μm. The simulation is halted if the cell moves to a distance 1.1*a* away from the top channel. The second example assumes that the cell has a Clausius−Mossotti factor of −0.4. Thus, the cell experiences negative dielectrophoresis and thus a repulsive force. It tends to move away from the electrodes. Simulations are performed using start time of 0 s, and end time of 5 s, with an initial velocity of 0 m s^{-1}. Three initial positions have been considered at different elevations of $y = 3.5$, 12.5, and 21.5 μm, respectively, with x fixed at 10 μm. The simulated cell trajectories in the xy-space for both examples are shown in Figure 5.

For cells experiencing positive dielectrophoresis, the simulation result indicates that cells move relatively slowly in the initial time steps and move significantly fast in the later time steps. The cell is attracted to the edge of the energized electrode. In contrast, cells experiencing negative dielectrophoresis move faster in the initial time steps but significantly slower in the later time steps. Note that the edge of the energized electrode exhibits the highest dielectrophoretic force; see Figure 3c. When a cell is near the top electrode, the electric field gradients are large; thus, the dielectrophoretic force acting on the cell is also large. Therefore, cells on positive dielectrophoresis experience a rapidly increasing attracting force toward the top electrode, and this attractive force will ultimately immobilize cells on the top electrode. In contrast, cells on negative dielectrophoresis experience a rapidly decaying repulsive force away from the top electrode. Such force distribution also causes cells at a higher y-elevation to travel faster or a longer distance compared to cells at a lower y-elevation.

This simulation result indicates that, by observing the nature of the cells motion, we can differentiate whether a cell is experiencing positive dielectrophoresis or negative dielectrophoresis. For cells experiencing positive dielectrophoresis, their trajectory is characterized by an accelerating motion followed by final immobilization at the energized top electrode, and this motion occurs in a fraction of a second. For cells experiencing negative dielectrophoresis, their trajectory shows a decelerating motion and they travel for several seconds before the motion is exhausted. These behaviors are unique to the moving dielectrophoresis system, which allows cells to be separated based on their dielectrophoretic affinity.

In practical application of the moving dielectrophoresis, the x-directional motion is more important and pronounced than the y-directional motion, since cells are separated from each other based on their horizontal traveling distances.

Effect of Various Parameters. The model can be used to analyze the behavior of the moving dielectrophoresis system, and for subsequent optimization of the design and control parameters to achieve high selectivity and throughput in cell separation. We have studied the effect of various key parameters to the x-directional motion of the cells. These parameters include cell initial position, applied voltage, electrode width, interelectrode gap, microchannel height, number of energized electrodes, cell size, and Clausius−Mossotti factor. Briefly, the results indicate that changing the electrode width, number of energized electrodes, and interelectrode gap does not significantly change the cell trajectory. Since these parameters also represent the distance that a cell has to travel before reaching the next electrode, they have to be minimized in enhancing the performance of a moving dielectrophoresis system. In general, since the cell motion is directly affected by the strength of the dielectrophoretic force, parameters that have positive correlation with the dielectrophoretic force would increase the cell travel distance and speed. In particular, increasing the applied voltage, decreasing the microchannel height (but not to the extent of increasing the drag force excessively), and increasing the absolute value of the Clausius−Mossotti factor, would increase the travel distance of a cell. A comprehensive discussion on the effect of these parameters is available in the Supporting Information.

COMPARISON WITH EXPERIMENTAL OBSERVATIONS

Experiments were carried out by energizing a single top electrode for ∼5 s with an applied voltage of ∼10 V peak-to-peak at an electrical frequency of 2 MHz. The viable yeast sample and nonviable yeast sample, *Saccharomyces cerevisiae* (strain ATTC 18824), were used separately. Each viable and nonviable yeast samples were suspended in 250 mM mannitol solution (M-9546 D-mannitol, Sigma), where the conductivity was adjusted to 305 μS/cm by adding sodium chloride. The top electrode width was 10 μm, and the microchannel height was ∼25 μm. At these operating conditions, the Clausius−Mossotti factors for the viable and nonviable yeast cells were estimated to be 0.42 and −0.34, respectively. Thus, the viable yeast cells represented particles experiencing positive dielectrophoresis, whereas the nonviable yeast cells represented particles experiencing negative dielectro-

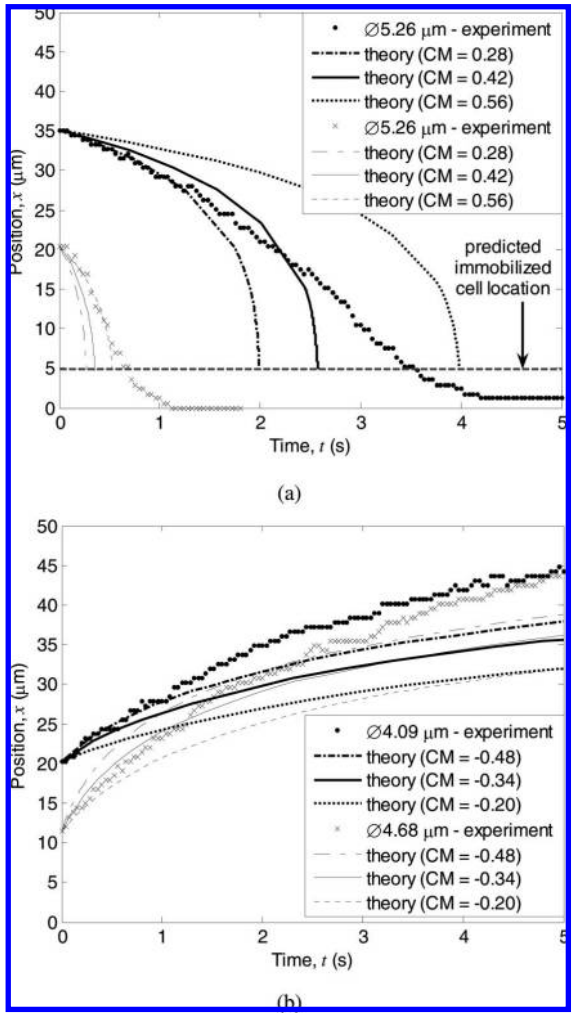

Figure 6. Comparison of experimental results with theoretical predictions. Experimentally, two cells at different locations were selected for each scenario. Simulations were run using three different values of Clausius−Mossotti (CM) factor. (a) Viable yeast cells experiencing positive dielectrophoresis. (b) Nonviable yeast cells experiencing negative dielectrophoresis.

phoresis. The motion of the cells was recorded through a CCTV camera (Sony ExwaveHAD SSC-DC58AP) using a commercial video tape recorder. The analog video was converted to digital video files using the Movie Studio EzCoder 3.0 program. The final digital video files had 25 frames/s. The cells trajectories were traced using the Manual Tracking plug-in of the image processing software ImageJ. The diameter of the yeast cells was measured in the image with two repetitions (a total of three readings). The detail equipment and experimental setup are contained in Kua et al.[10]

The trajectories of viable and nonviable yeast cells were plotted in Figure 6a and Figure 6b, respectively. Experimentally, two candidates with different initial *x*-positions were selected for each viable and nonviable yeast cells. The initial *x*-positions of the cells can be deduced from the plots. The diameter of the cells is shown in the corresponding legend. Numerically, for each cell, three different Clausius−Mossotti factors were employed in the simulations. For viable yeast cells, the Clausius−Mossotti factors employed were 0.28, 0.42, and 0.56. The values of 0.28 and 0.56 provided an upper and lower bounds to cater for experimental variations and uncertainties. Similarly, for nonviable yeast cells, the Clausius−Mossotti factors employed were −0.20, −0.34, and −0.48. The simulations were performed using a start time of 0 s, and an end time of 5 s, with an initial zero velocity. The yeast cells were assumed to have a density of 1087 kg m^{-3}. Since the video was recorded on the *xz*-plane, the *y*-position of the cells in the microchannel was not known. The cells were assumed to have an initial *y*-position of 12.5 μm in calculating the theoretical trajectories. The trajectories of the cells for the initial *y*-position of 5 and 20 μm, respectively, would be smaller than the range bounded by varying the Clausius−Mossotti factor. Therefore, the theoretical cell trajectories due to the variation in the initial *y*-position were not included in the plots.

Qualitative agreement was obtained between the experimental observations and the simulated results. Both the experimental and simulated trajectories of the yeast cells exhibited the same trend. For viable yeast cells, which experience positive dielectrophoresis, the experimental results show that they moved in an increasing acceleration toward the energized electrode, before slowing down and finally immobilized at the energized electrode; see Figure 6a. This immobilization behavior was due to the attractive force experienced by the viable yeast cells.

For nonviable yeast cells, which experience negative dielectrophoresis, the experimental trajectories showed a rapid increase in velocity at the initial time frame, and a slower increase in velocity at a later time frame, which are also predicted by the simulations. See Figure 6b. In contrast to the viable yeast cell, which experiences immobilization on the electrode, the nonviable yeast cell is never immobilized on the electrode due to the repulsive force by the electrode on the nonviable cell. The effect of the cell size was relatively minimal. Both experimental observation and simulation indicates that nonviable yeast cells of different sizes approached a similar final location although starting at different initial *x*-positions.

However, there were at least two phenomena not captured by the model. First, the viable yeast cells were predicted to have a steep increase in velocity when they were near to the energized electrode. Instead, the viable yeast cells approached the energized electrode rather linearly before slowing down and finally immobilized at or near the energized electrode. Second, the nonviable yeast cells traveled farther than predicted by the theoretical model. Noting that the Clausius−Mossotti factor of −0.50 is the theoretical maximum negative value that is possible, the trajectories traced by the Clausius−Mossotti factor of −0.48 were still below the experimental trajectories.

A possible explanation to these discrepancies is that the electrohydrodynamic effect was not taken into account in the model. Such electrohydrodynamic effect arises from the interaction of the applied electric field with the fluid medium, where the fluid medium is polarized, resulting in an induced fluid flow. As a result, the motion of the cells is affected by this additional induced fluid flow. If the induced fluid flow is in the same direction as the dielectrophoretic force, the cells would travel farther than predicted, and vice versa. A localized fluid flow around the edge of the energized electrode would prevent the cells experiencing positive dielectrophoresis to be immobilized there and, thus,

exhibited tailing off behavior as shown in Figure 6a. A fluid flow moving in a direction away from the energized top electrode would propel a cell experiencing negative dielectrophoresis to travel further, as shown in Figure 6b. Further studies are required to confirm this hypothesis.

CONCLUSION

A mathematical model describing the cell motion and trajectory in moving dielectrophoresis for cell separation and transportation has been presented. The model takes into consideration the four dominant forces acting on a cell, including dielectrophoretic force, fluid drag, gravitational force,and buoyancy force. A MATLAB algorithm, with all the associated files, is written for the tedious task of solving numerically the equation of motion for the cell trajectory. The algorithm is available on request. Various parametric studies were performed. Results show that the distance a cell travels in the *x*-direction is sensitive to the initial *y*-position when the cell is near to the origin. It is also sensitive to the cell Clausius−Mossotti factor, but its effect diminishes at higher polarization magnitude. Other factors such as size, applied voltage, interelectrode gap, and microchannel height are important. In contrast, the cell travel distance is not sensitive to the electrode width and the number of electrodes energized. Qualitative agreements were obtained between simulated and experimental results, showing the unique nature and differences of trajectories for cells experiencing either positive or negative dielectrophoresis. Discrepancies between predictions and experimental observations could be explained by the electrohydrodynamically induced fluid flows, which have not been included in the model.

ACKNOWLEDGMENT

This work was supported by the Singapore−MIT Alliance research fund. The authors thank Prof. Ronald Pethig for valuable discussion on yeast cell modeling.

SUPPORTING INFORMATION AVAILABLE

A text file discussing the effect of various key parameters on cell motion. This material is available free of charge via the Internet at http://pubs.acs.org.

Received for review December 17, 2007. Accepted May 14, 2008.

AC800947E